

Fig. 3: MAVIREC ML inference for fast IR drop analysis.

using 3D convolutions for capturing switching activity.

- A novel recommender system that uses fast ML inference to select hundreds of slices when compared to conventional flow that selects 3–5.
- An accurate system for profiling long vectors (≈ 100 -cycles), maximizing regional coverage, on industrial scale designs in 30 minutes ($4\times$ speedup vs. industrial flow).

II. MAVIREC FOR VECTORED DYNAMIC IR ESTIMATION

The core engine in the proposed flow in Fig. 1 (right), for both the vector profiling and rail analysis, is MAVIREC’s ML inference scheme. The scheme first performs feature extraction and then uses a trained model for IR drop estimation.

A. Feature extraction

The MAVIREC ML model uses two types of features, differentiated by the method in which they are represented:

- Instance-level power and effective distance to via stack
- Spatial and temporal full-chip tile-based power maps, and spatial time-invariant resistance maps

Table I lists the features used in our ML model, encapsulating power information, the local PDN topology, and switching activity. We first extract these features from the design environment. Fig. 3 shows our two-part process of extracting instance-level features (dotted black box) and generating 2D spatial and temporal feature maps (blue box).

Instance-level feature generation We run three standard tools highlighted in the green and yellow boxes of Fig. 3 to extract instance-level information from the design:

- 1) a power analysis tool to generate a per-instance switching (p_s), internal (p_i), and leakage power (p_l) report.
- 2) a parser tool to extract from the DEF (a) instance locations (b) effective distance of an instance to power rail via stacks in the immediate ($5\mu\text{m}$) neighborhood. The effective distance metric is: $r^{-1} = d_1^{-1} + \dots + d_V^{-1}$ where d_i is distance from the instance of the i^{th} of V via stacks.
- 3) a tool that extracts the times when instances toggle, from the VCD file (industry-standard format) for each slice.

Similar to [5], in addition to p_l , p_s , p_i , and r , there are three other instance-level features which are derived from these. The toggle rate scaled and total power are given by $p_r = p_l + \tau_i(p_s + p_i)$ and $p_{tot} = p_l + p_s + p_i$ respectively, where τ_i is the average toggle rate of the instance in the specified slice. The overlap power p_{ol} sums up the p_r of all neighboring instances that share the same timing window.

Generation of 2D spatial and temporal maps as features

The map creation step performs a spatial and temporal decomposition (Fig. 3 (blue box)) of the per-instance features in a

TABLE I: MAVIREC’s features for dynamic IR prediction where the lowercase symbols are instance-level and uppercase are at the tile-level.

List of all features	
Internal power: p_i, P_i	Overlap power: p_{ol}, P_{ol}
Leakage power: p_l, P_l	Total power: p_{tot}, P_{tot}
Switching power: p_s, P_s	Effective distance: r, R
Toggle rate scaled power: p_r, P_r	Toggle power at each time step: p_t, P_t
Ground truth training labels	
Instance-level IR drop: IR_i , NA (heat map only)	

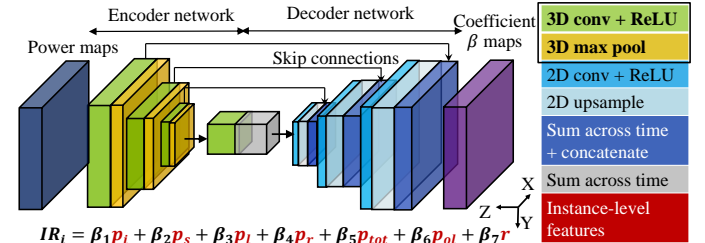


Fig. 4: MAVIREC: 3D convolution and regression model based U-Net architecture for dynamic IR drop prediction.

similar manner as [5]. For the spatial-tile based features, we associate the location of each instance with its corresponding power/effective distance attributes to create 2D distributions of these attributes at a fixed granularity (*tile size*). We choose a tile size of $W_t = 2.5\mu\text{m} \times L_t = 2.5\mu\text{m}$; a design of size $W_c \times L_c$ corresponds to an “image” of $W (= W_c/w_t) \times L (= L_c/l_t)$ tiles. For each instance-level feature in Table I, its tile-based counterpart adds per instance power-related features, and takes the maximum effective distance over all instances, in the tile.

For dynamic IR drop analysis, we also consider temporal power maps. To generate p_t (the power of an instance at each time step) we divide the n -cycle time window into $n \times t$ time steps, where n is usually predetermined by the designer as the window size of interest (we use $n = 20$) and t is a hyperparameter to be tuned. It was observed that $t = 5$ provided the best results with MAVIREC. The power of an instance at time step j is given by: $p_t(j) = \sum_{i=1}^{100} p_i + b_j(p_i + p_s)$ where the Boolean variable b_j is 1 only if the instance toggles at time step j . Thus, we create time-decomposed power maps at each time step using the toggle information and timing windows.

All features in Table I are normalized between 0 and 1 and are inputs to the trained ML model. Normalization scales the input by a predetermined constant that is defined for the technology, e.g., the maximum supply voltage or current.

B. MAVIREC architecture

Fig. 4 shows the structure of MAVIREC for vectored dynamic IR drop estimation, with layer descriptions provided in the legend. It consists of two subnetworks for (i) encoding (downsampling) and (ii) decoding (upsampling), with skip connections between the networks. The skip connections use a concatenation layer to incorporate information from an early layer into a deeper stage of the network, skipping intermediate layers, and appends it to the embedding along the z -direction. This architecture is based on fully convolutional (no fully connected layers) U-Net models [8] used for image segmentation. The fully convolutional nature of U-Nets makes them fast and they are designed to be input-image-size-independent. The

convolutional and max-pool layers of the U-Net capture local and global spatial neighborhood features.

The work in [7] uses U-Nets for estimating *static* IR drop. However, for reasons listed in Section I, this model is not suitable for vectored dynamic IR drop analysis. In addition, typical for real workload vectors, cells switch at only a few spatial and temporal locations. This makes the temporal power map P_t extremely sparse and difficult to capture in the zero-dominant data. As shown in Section IV-A, merely accounting for these sparse temporal features is not sufficient, and the ML architecture must be able to capture these sparse local changes accurately. There are two key differences from the U-Net in [7] that are crucial for overcoming its limitations:

- *3D convolutional layers* (green layers) in the encoding path captures temporal simultaneous switching activity.
- *regression-like layer* at the end of the decoder that incorporates instance-level input features and the instance-level IR drop IR_i (equation in Fig. 4) using β_i , the coefficient matrix predicted by the U-Net like structure.

3D convolutional layer in the encoder Unlike a 2D convolutional layer that uses all input channels during convolution, a 3D convolutional layer restricts the number of channels to the specified filter size in the channel dimension, thus considering only a small local window of channels. When all the temporal power maps are taken together as channels in a regular 2D convolutional layer, due to zero-dominance in the data, the model fails to capture key non-zero toggle activity regions and time steps. Intuitively, a small local window of channels which a 3D convolutional layer considers would better capture simultaneous and sparsely-distributed switching activity. Therefore, MAVIREC uses a $3 \times 3 \times 3$ filtered 3D convolutional layer in the encoding path instead of a regular 3×3 2D convolutional layer as in U-Net (green layer in Fig. 4). MAVIREC has $n \times t + 7$ tile-based channels (Table I):

- $n \times t$ temporal power maps (P_t) to the encoder network
- 7 tile-based spatial features ($P_i, P_l, P_s, P_r, P_{ol}, P_{tot}, R$) where $n \times t$ represents the number of time steps (Sec. II-A).

We will show in Section IV-A that a 2D convolution model does not accurately capture simultaneous switching compared to 3D convolution. MAVIREC consists of four 3D convolutional layers and three 3D max pool layers in the encoder network and four 2D convolutional layers and three upsampling layers in the decoder network. Since the decoding path uses 2D convolutions, the interface between the 3D embedding in the encoder and the 2D embedding in the decoder sums up the embedding along the temporal dimension (dark blue boxes in Fig. 4) through concatenation/skip connections.

Regression-like layer in the decoder To enable IR drop prediction at a per-instance level, MAVIREC leverages a regression-like layer at the end of the decoder path that uses instance-level input features and multiplies them with the predicted coefficients (β_i) by the U-Net-like structure in Fig. 4. The predicted coefficients are based on the $n \times t + 7$ spatial and temporal tile-based channels as input. The coefficient predicted for every tile is then multiplied with the per-instance feature values defined in Sec. II-A. This architecture provides three key advantages over prior ML-based solutions [5], [7]:

- 1) *Improved transferability* compared to prior art, as the model uses both instance-level features directly and tile-

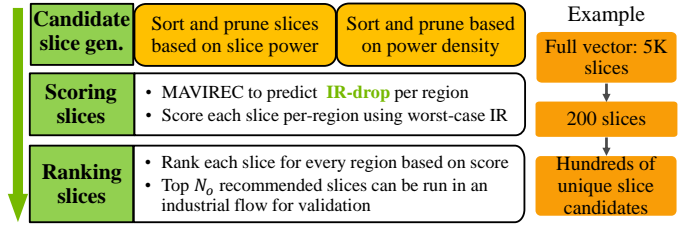


Fig. 5: MAVIREC vector profiling which uses ML inference under the hood to generate hundreds of ranked candidates.

level features to predict IR drop at a per-instance level. The instance-based features help capture fine-grained variations in the data that is otherwise lost due to the averaging nature of U-Net convolutions. Instead of learning the IR drop values directly as in [5], [7], the U-Net-like structure learns the relationship (β_i) between the features and the IR drop values, which is universal across designs.

- 2) *Improved instance-level IR drop predictability* compared to prior art, which is useful for applications such as IR-aware STA and instance-based IR drop mitigation.
- 3) *Model interpretability* as the predicted coefficients are the weights associated with each feature. The coefficients correspond to feature sensitivity, and allow designers to assess the root cause of an IR drop violation.

A trained MAVIREC model is reusable, without the need for retraining when faced with new designs/vectors for a given technology. Although the prediction is on an instance level granularity, it is not necessary to loop through all instances to estimate the IR drop. Instead, we define a location matrix that creates a mapping between each instance and its corresponding tile-based coefficient. This mapping eliminates the loop by using element-wise matrix multiplication which is accelerated on GPUs (details have been omitted due to space constraints).

III. MAVIREC FOR VECTOR PROFILING

The input vectors in real workloads can typically have hundred of thousands of cycles, which corresponds to ~ 5000 slices. These slices of 20 cycle windows each form inputs to the rail analysis step for IR drop estimation. Given the runtimes of industrial flow rail analysis, it is near-impossible to run rail analysis on all slices. Using a brute force approach, where MAVIREC is used as a fast IR drop estimator, is not a viable solution either as each inference involves extracting temporal features at recurring runtime costs (see Fig. 3) for each of the 5000 slices. This calls for techniques to select a large set (70–200) of candidate slices that represent the design and worst-case IR drop vector. In contrast, industrial flows are limited to 3–5 slices due to IR analysis run-times.

Fig. 5 and Algorithm 1 detail MAVIREC’s vector profiling flow. The inputs are per-instance leakage, switching and internal power p_l, p_s , and p_i , region size $w \times l$, chip size $W_c \times L_c$, the number of slices to select at each of the two stages of candidate generation given by N_a and N_r , and N_o is the number of top rank slices to report at the end of the profiling. The number of regions in the design is given by $W_r \times L_r$ where $W_r = W_c/w$ and $L_r = L_c/l$.

Inspired by classical ML recommender system [9] nomenclature, our method (Fig. 5) is a three-step process which consists of (i) candidate generation (two stages), (ii) scoring,

Algorithm 1 MAVIREC’s algorithm for vector profiling

Input: Per instance internal, switching, and leakage powers p_i , p_s , p_l ; Per instance toggle count T_c ; Number of slices to select N_a , N_r , and N_o ; Region size $w \times l$; Chip dimensions $W_c \times L_c$; List of all candidate slices in vector C_N ;

Output: Candidate slices for worst-case IR drop C_{N_o}
IR drop map IR_{chip, N_o} of the C_{N_o} candidates

```

1:  $W_r = \frac{W_c}{w}$  and  $L_r = \frac{L_c}{l}$ 
2: // Candidate slice generation starts here
3: // Stage 1: sort and eliminate based on average slice power
4: for each slice  $c$  in  $C_N$  do
5:    $P_{slice}[c] = \sum_{\forall \text{instances}} \left[ p_l + \frac{T_c[c]}{20} (p_s + p_i) \right]$ 
6: end for
7:  $C_{N_a} =$  Top  $N_a$  candidate slices with highest value in  $P_{slice}$ 
8: // Stage 2: sort and eliminate based on average regional power
9: for each region  $r_i$  in  $W_r \times L_r$  do
10:  for each candidate slice  $c$  in  $C_{N_a}$  do
11:     $P_R[r_i][c] = \sum_{\forall \text{instances} \in r_i} \left[ p_l + \frac{T_c[c]}{20} (p_s + p_i) \right]$ 
12:  end for
13:   $C_{N_r}[r_i] =$  Top  $N_r$  candidate slices with highest value in  $P_R[r_i]$ 
14: end for
15:  $C_{N_c} =$  Unique candidates from  $C_{N_r}$ 
16: // Candidate scoring and ranking starts here
17: for each slice  $c$  in  $C_{N_c}$  do
18:   $F[c] =$  Feature_extraction( $c$ )
19:   $IR_{chip} =$  ML_inference( $F[c]$ )
20:  for each region  $r_i$  in  $W_r \times L_r$  do
21:     $IR_{score}[r_i][c] = \max(IR_{chip}[c])$  in  $r_i$ 
22:  end for
23: end for
24:  $n = 1$ 
25: while  $n \leq N_o$  do
26:   $r_i, C_{N_o}[n] =$  Top  $N_o$  unique candidates, regions with highest  $IR_{score}$  values
27:   $IR_{chip, N_o}[n] = IR_{score}[x][C_{N_o}[n]] \forall x \in W_r \times L_r$ 
28:   $n++$ 
29: end while

```

and (iii) ranking. At each stage of candidate generation, we prune out slices based on average power first and regional-power next. We score the remaining slices using the worst-case IR drop as a metric and rank them using a technique that maximizes regional coverage. Fig. 5 displays an example of candidate generation where a number of slices are pruned out of the set at each stage.

Candidate slice generation: This step of the vector profiling flow consists of two stages (Lines 4–15).

First stage In each of our vectors, we observe that there are thousands of slices with near-zero switching activity. Therefore, in the first stage of candidate generation we sort and prune the set of slices based on the average power of each slice, as shown in lines 4–7. Pruning at this stage saves time by preventing feature extraction for slices that are obviously not IR-critical. The pruned and sorted list, C_{N_a} , has hundreds of potential candidates to move on to the next stage of our flow (much more than 3–5 in industrial flows).

Second stage Since the IR drop of an instance depends on the switching activity of an instance and its neighborhood, power per region is vital for IR drop. Therefore, in the second stage of candidate generation (lines 9–15), we calculate the power per region in the design and then rank the C_{N_a} candidate slices in each region. We then extract the top N_r from each region. This results in a list, C_{N_r} , of $N_r \times W_r \times L_r$ candidate slices and C_{N_c} is the list of N_c unique candidates from C_{N_r} .

Candidate slice scoring and ranking At this step, we score each of the N_c (hundreds) generated candidates based on worst-case IR drop of each slice in each region. For this, we take each candidate slice C_{N_c} and generate all the required features required (Table I) for the ML inference in line 18. The inference engine in MAVIREC is then used to generate a full-

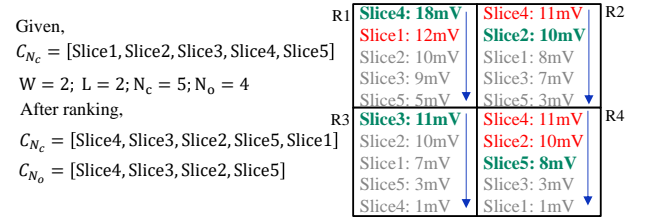


Fig. 6: Scoring and ranking scheme for C_{N_c} candidates.

chip IR drop as detailed in line 19 and Section II-B. The worst-case IR drop across the chip is used to score each slice. This results in $N_c \times W_r \times L_r$ score values in IR_{score} (line 21). We then rank each candidate based on the worst-case IR drop and record its corresponding region (line 26). Only those unique N_o candidates that correspond to the worst-case IR drop of a previously uncovered region are stored in C_{N_o} .

Fig. 6 shows the scoring and ranking scheme for a demonstrative example of a chip with four regions R1–R4 and $N_c = 5$ generated candidate slices. For each region, the slices are ranked in decreasing order of the score/worst-case IR drop in the region. The unique slice from each region with the highest score is selected. The worst-case IR drop of the design is 18mV and corresponds to Slice 4 in R1. The next highest IR drop is Slice 1, with 12mV in R1. However, since R1 has already been covered, we do not need to report Slice 1. The next highest IR drop is Slice 3 in R3 and Slice 4 in R2 with 11mV. In this case, Slice 4 has already been covered by R1, which makes Slice 3 the next highest rank. We repeat the same process until we cover all $W_r \times L_r$ regions. In this way, we ensure to report candidates based on worst-case IR drop while maximizing regional coverage. We also report the IR drop maps of C_{N_o} candidate list (line 27).

Computational complexity Our candidate generation step is of the order of $O(N \log N_a) + O(W_r L_r N_a \log N_r)$, for the first and second stage respectively. The $\log N_a$ and $\log N_r$ come from keeping track of the top N_a and N_r candidate slices which are small user-defined upper-bounded numbers that do not change across designs and tests. We use $N_a = 200$ and $N_r = 5$ which changes the complexity to $O(N) + O(W_r L_r)$. In practice, N , the number of slices in the vector, are of the order of the hundreds of thousands while $W_r L_r$, the number of regions in the design, is in the order of thousands. Therefore, we have a complexity of $O(N)$, linear in the number of slices in the vector.

IV. RESULTS AND DISCUSSIONS

In our experiments, we use four industrial designs, D1–D4, implemented in a sub-10nm FinFET technology and three multi-cycle vectors, T1–T3, per design. Table II summarizes the designs and tests used in our training set. The data available to us were taped out designs in an industrial setting with low IR drop values. Therefore, we use a threshold of 8mV to classify IR-critical regions. The model is trained end-to-end using golden per-instance IR drop labels obtained from an industrial flow using commercial tools. We evaluate MAVIREC with *leave one out cross validation*, where in each training run one design and its tests are omitted from the training set. These are implemented in a PyTorch 1.6 [10] framework on an 8-core CPU machine with 256GB RAM and

TABLE II: Summary of designs and vectors used in MAVIREC experiments with a tile size of $2.5\mu\text{m} \times 2.5\mu\text{m}$.

Design	#inst. (mill.)	T1		T2		T3	
		%IR -critical regions	Toggle rate	%IR -critical regions	Toggle rate	%IR -critical regions	Toggle rate
D1	3.26	13.66	0.054	16.04	0.062	8.98	0.041
D2	2.19	4.60	0.043	4.24	0.040	3.59	0.038
D3	2.18	4.28	0.040	4.31	0.038	3.88	0.038
D4	2.43	16.88	0.085	10.68	0.087	13.00	0.089

TABLE III: Performance of MAVIREC ML inference compared to an industrial flow. RMSE and MAE at instance-level granularity and % accuracy as a binary classifier at region-based granularity.

		RMSE, MAE (mV)		% Accuracy 1x1, 6x6				RMSE, MAE (mV)		% Accuracy 1x1, 6x6	
D1	T1	4.44	3.3	89.09	84.98	D3	T1	3.02	26.8	96.26	93.45
	T2	4.61	25.2	85.49	88.72		T2	2.99	22.4	96.12	92.89
	T3	3.91	30.2	92.93	88.93		T3	2.93	35.1	95.96	92.56
D2	T1	3.1	25.4	95.68	92.73	D4	T1	3.87	24.1	89.43	91.07
	T2	3.11	20.6	95.86	92.77		T2	3.38	24.7	90.27	93.62
	T3	2.99	21.8	96.08	92.19		T3	3.31	24.5	90.25	94.55

one NVIDIA Tesla V100GPU with 32GB RAM. We use an ADAM optimizer [11] for training and use an L_2 regularizer to prevent overfitting. The model takes 9 hours to train and is a one-time cost per technology. The trained model is transferable across both designs and vectors.

A. MAVIREC for IR drop prediction and classification

MAVIREC vs. industrial flow for IR drop We compare MAVIREC-predicted IR drop against a ground truth IR drop from an industrial flow. Similar to the industrial flow, MAVIREC predicts IR drop at a per-instance granularity. Table III shows the RMSE and max error for all the designs and tests and it is seen that the RMSE is very small ($<4\text{mV}$) and is within reasonable limits for instance-level applications such as cell-level IR drop mitigation and IR-aware STA.

The rest of the table depicts the performance of MAVIREC as an IR drop hotspot classifier on a per-tile basis, where a tile is considered hot if the average IR drop of all instances in that tile is greater than the threshold (8mV). We consider two different granularities, a 1×1 tile ($2.5\mu\text{m} \times 2.5\mu\text{m}$) and 6×6 tiles ($15\mu\text{m} \times 15\mu\text{m}$), and report the accuracy for each design and test. We obtain an average accuracy of 93.12% and 91.22% at the 1×1 and 6×6 granularities respectively. At 6×6 granularity we have an F1 score of 0.78, which despite the heavily imbalanced minority class ($<10\%$ in the dataset), still captures all large hotspots which are of interest to designers. This accuracy outperforms prior art (Section IV-A) and is sufficient for vector profiling (Section IV-B).

For a visual comparison of the IR drop hotspot map, we convert the instance-based IR_i to tile-based, taking the mean IR drop of all instances in a ($2.5\mu\text{m} \times 2.5\mu\text{m}$) tile. Fig. 7 shows the predicted and ground truth IR maps for a section of each design for test T1. The MAVIREC-predicted IR drop map captures all major hotspots relative to the ground truth. **MAVIREC versus ML-based IR drop classifiers** As a comparison to prior art, we implemented a maximum CNN structure similar to PowerNet [5]. To ensure a fair comparison, we make the following changes: (i) As the focus of PowerNet was vectorless IR drop estimation and does not support the use of multi-cycle switching activity, to adapt PowerNet, we take the average toggle rate from the vectors. (ii) PowerNet predicts

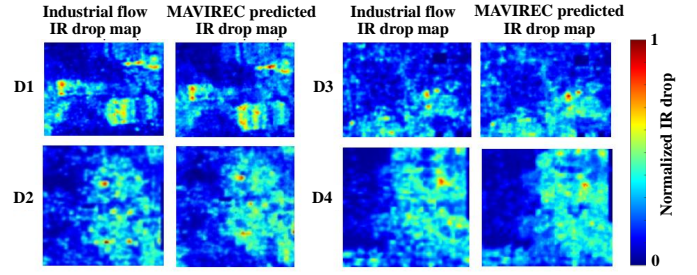


Fig. 7: Visualization of MAVIREC-predicted IR drop map and industrial flow IR drop map for all four designs.

IR drop on a per-tile ($1\mu\text{m} \times 1\mu\text{m}$) basis, while MAVIREC is on a per-instance basis. Therefore, MAVIREC generates a region-based IR drop, like PowerNet, by taking the mean of the predicted-IR drop of all instances in the tile.

We compare MAVIREC against two baseline ML models: (i) a vanilla U-Net, identical to MAVIREC except that it uses 2D convolutional layers, and (ii) a max U-Net, identical to PowerNet except that the CNN is replaced with a 2D convolutional U-Net with an output regression layer (Section II). The vanilla U-Net processes all time steps simultaneously while the max U-Net processes each time step separately. The max U-Net sets the final IR drop to the maximum IR drop for each instance across all time-steps. We train all models on the same dataset and tune the hyperparameters for optimal performance.

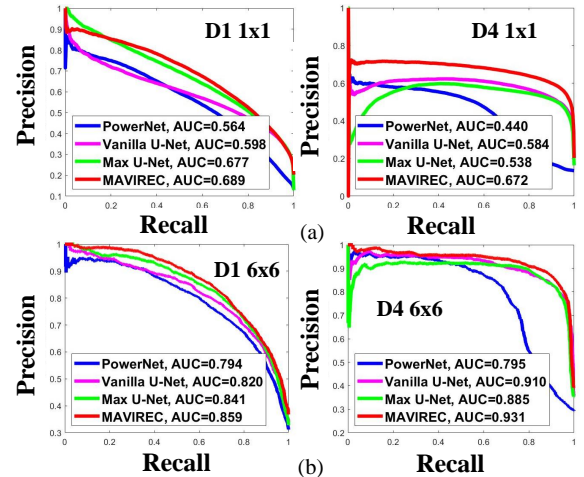


Fig. 8: Comparison of MAVIREC against PowerNet, Max U-Net, and 2D U-Net. Precision Recall curves showing MAVIREC's ability to predict the minority class on designs D1 and D4 (as representative examples) for a tile size of (a) 1×1 and (b) 6×6 tiles

The area under curve (AUC) of the precision-recall (PR) curve is a single value that demonstrates the ability of the classifier to predict the minority class, in a highly imbalanced dataset. A random classifier has a PR curve equal to the fraction of minority class in the dataset, while for a classifier that always predicts the majority class, the PR curve coincides with the x-axis. Fig. 8 shows that MAVIREC outperforms both PowerNet and baseline ML models in predicting the IR-critical class across designs with larger AUCs for 1×1 (Fig. 8(a)) and 6×6 (Fig. 8(b)) tile granularities. The 3D convolutional layers in MAVIREC capture the sparse switching activity of the vectors, but the vanilla and Max U-Net fail to do so due to their 2D convolutional nature.

TABLE IV: Runtime comparison of industrial flow and models.

Task	Industrial flow	PowerNet	Max U-Net	Vanilla U-Net	MAVIREC
Feature extraction	3 hours	17 mins			
ML inference		5 mins	7.2s	1s	3s

In addition to accuracy, inference speed is critical to enable model scalability and to check a large number of cycles rapidly. Table IV compares the inference times of an industrial flow, PowerNet, MAVIREC, and baseline ML models. The runtimes are reported on D1 with 3.2 million instances and includes the inference and feature extraction time. Accounting for the feature extraction time allows a fair comparison against the industrial flow. The total runtime is 18 minutes, which gives a $10\times$ **speedup** over the industrial flow rail analysis. Most of the 18 minutes is spent in extracting the required features and the distribution of runtimes for each feature is listed in Fig. 3, and the inference alone is less than **3s**. MAVIREC is $2\times$ faster than max-U-Net and $100\times$ faster than PowerNet in pure inference. The vanilla U-Net is faster than MAVIREC but is less efficient in predicting hotspots (Fig. 8).

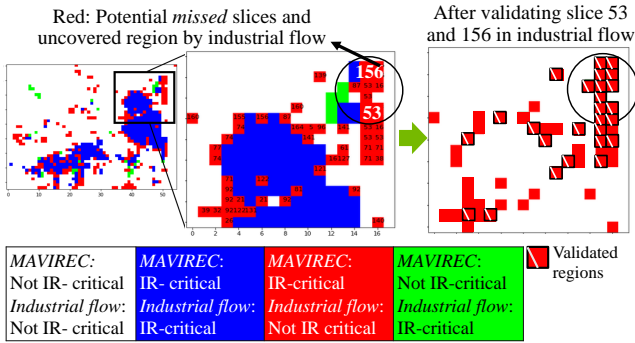


Fig. 9: Regional coverage comparison of MAVIREC’s 168 candidate slices against 3 candidate slices from industrial flow. Validation of the largest industrial flow-uncovered IR-critical regions on design D2 as a representative example.

B. MAVIREC for vector profiling

Quality of MAVIREC-recommended vectors The input vectors to our profiling algorithm (Section III) have about 100,000 clock cycles \approx 5000 slices. For $N_a = 200$, $N_r = 5$, $N_o = 3$, and $w \times l = 15\mu\text{m} \times 15\mu\text{m}$ (6×6 tiles), the algorithm generates $N_c \approx 100$ candidate slices per vector. Fig. 9 shows the coverage comparison between the industrial flow-generated top-3 candidate slices and 168 MAVIREC-recommended slices on a representative design D2. Fig. 9 (leftmost) compares the regional coverage. The middle picture shows the part of the design with the largest industrial flow-missed IR-critical spots (set of red regions). The numbers on the red regions indicate slice IDs (a numeric ID number for identifying each unique slice of the testbench) that resulted in those regions being reported as IR critical by MAVIREC. These are a set of *missed* slices and we validate slice IDs 53 and 156 using an industrial flow. The rightmost map shows black-outlined and white-dashed red regions which were validated to be IR-critical and the rest of the red regions are not validated. In the four designs we consider, each has ≈ 30 unique missed slices. It would be near-impossible to validate each missed slice by running industrial flow (ground truth) IR drop analysis, given

TABLE V: MAVIREC vs. industrial flow recommended slices.

Design, Test	Industrial flow profiling		MAVIREC profiling		Comparison			
	N_c	#IR-critical regions	N_c	#IR-critical regions	#Regions reported IR-critical by both	% Regions uncovered by MAVIREC	% Regions uncovered by industrial flow	#Unique slice IDs of missed regions
D1, T1	3	1163	133	1531	1093	1.7	10.8	30
D2, T1	3	422	168	550	383	1.6	6.9	36
D3, T1	3	369	166	553	329	1.7	9.4	26
D4, T1	3	682	73	786	672	0.4	4.5	11

storage (30GB per slice), time (3 hours per slice), and license limitations. Therefore, we limit our validation to missed slices with the largest uncovered region cluster.

Table V lists the number of candidates, N_c , generated for each design for the test T1. For each of the designs we consider and for a region size of 6×6 tiles, we have 70–170 candidate slices generated while a industrial flow generated three slices. MAVIREC provides a large coverage by reporting an average of $\sim 5\%$ of the regions as potentially uncovered by the industrial flow and has less than 1.7% false negatives. **MAVIREC vector profiling runtimes** MAVIREC is able to provide high-quality recommendations for a 100K-cycle vector in 30 minutes while the industrial flow takes up to 2 hours.

V. CONCLUSION

We propose MAVIREC: a fast and accurate vector profiling system that recommends a set of worst-case IR drop switching patterns using an ML-based IR drop estimation. MAVIREC can profile hundred thousand-cycle vectors in under 30 minutes ($4\times$ speedup vs. industrial flows) on industrial designs and captures regions that were missed by industrial flows. MAVIREC’s inference for IR drop estimation is $10\times$ faster than industrial flows at the cost of a mere 4mV error. While this work focused on vectored dynamic IR drop analysis, the ML inference engine can be adopted for both vectorless dynamic and static IR drop analysis.

REFERENCES

- [1] N. Ahmed, M. Tehranipoor, and V. Jayaram, “Transition delay fault test pattern generation considering supply voltage noise in a SOC design,” in *Proc. DAC*, 2007.
- [2] V. A. Chhabria *et al.*, “Template-based PDN synthesis in floorplan and placement using classifier and CNN techniques,” in *Proc. ASP-DAC*, 2020.
- [3] Y.-C. Fang *et al.*, “Machine-learning-based dynamic IR drop prediction for ECO,” in *Proc. ICCAD*, 2018.
- [4] C. Ho and A. B. Kahng, “IncPIRD: Fast learning-based prediction of incremental IR drop,” in *Proc. ICCAD*, 2019.
- [5] Z. Xie *et al.*, “PowerNet: Transferable dynamic IR drop estimation via maximum convolutional neural network,” in *Proc. ASP-DAC*, 2020.
- [6] K. Acharya and N. Dhanwada, “Learning-based approach for early power grid analysis in high performance microprocessor designs,” Presentation at DAC (User Track), 2020.
- [7] V. A. Chhabria *et al.*, “Thermal and IR drop analysis using convolutional encoder-decoder networks,” in *arXiv:2009.09009 [cs.ar]*, 2020.
- [8] O. Ronneberger, P. Fischer, and T. Brox, “U-Net: Convolutional networks for biomedical image segmentation,” in *Proc. Int. Conf. Med. Image Comput. Comput.-Assisted Intervention*, 2015.
- [9] P. Covington, J. Adams, and E. Sargin, “Deep neural networks for YouTube recommendations,” in *Proc. ACM Conf. Recomm. Sys.*, 2016.
- [10] A. Paszke *et al.*, “PyTorch: an imperative style, high-performance deep learning library,” in *Proc. NeurIPS*, 2019.
- [11] D. Kingma and J. Ba, “ADAM: A method for stochastic optimization,” in *Proc. ICLR*, 2014.